CARNEGIE INSTITUTE OF TECHNOLOGY

DEPARTMENT OF ELECTRICAL ENGINEERING

PITTSBURGH 13, PENNSYLVANIA

EDDY-CURRENT PHENOMENA IN FERRO-MAGNETIC MATERIALS

H. M. McCONNELL

MAGNETIC AMPLIFIERS - TECHNICAL REPORT NO. 14

WORK PERFORMED UNDER OFFICE OF NAVAL RESEARCH CONTRACTS
N7 ONR 30305 AND 30308 - PROJECT NO. 975-272 AND 275

MAGNETIC AMPLIFIERS - TECHNICAL REPORT NO. 14

EDDY-CURRENT PHENOMENA IN FERRO-MAGNETIC MATERIALS

by H. M. McConnell

Work performed under Office of Naval Research Contracts N7 ONR 30306 and 30308, Project No. 975-272 and 275.

Synopsis

The need for an adequate method to account for eddy currents in magnetic materials has been apparent for some time, especially since the development of high quality magnetic amplifiers. This paper correlates existing theories of eddy currents in saturated iron. In particular an approach originally suggested by A. G. Ganz is treated in a comprehensive mathematical analysis based on classical field theory.

This approach seems well suited to account for the influence of eddy currents upon the transfer characteristics of magnetic amplifiers using "sharp" core materials. It is shown that the method is useful also in more conventional applications, such as inductive and conductive heating of solid iron.

Department of Electrical Engineering
Carnegie Institute of Technology
Pittsburgh 13, Pennsylvania
August, 1953

EDDY-CURRENT PHENOMENA IN FERRO-MAGNETIC MATERIALS

Introduction

Interest in eddy currents in solid iron masses has kept pace with the development of electromagnetic devices generally. The first problems arose in the design of eddy current brakes for flywheels. Then the use of iron wire for telephone lines and iron rails for the supply of power to alternating current locomotives led to new problems. It was recognized that the saturation of the iron was an important factor, and many authors have presented their theories to take saturation into account. Following the appearance of Rosenberg's work, others have made an academic problem of substantiating it or elaborating upon it. Recently the damping effect of eddy currents in the solid yokes and pole pieces of direct current machines has become important. Still more recently, it has been recognized that the saturation effect is important in computing the core losses in thin steel or alloy sheets. Representative references in the field are listed in the bibliography (references 1 to 6).

A new method for computing the effect of saturation has been suggested by A. G. Ganz (7). The method seems to be a significant departure from other efforts to account for magnetic non-linearity in iron. Many attempts to handle the problem mathematically have introduced the non-linearity as a sort of correction to the linear theory, always keeping in mind that the treatment should reduce to the linear theory as a special case. An almost exact parallel can be found in the various approaches to the non-linear problem of the magnetic amplifier. On the one hand there is the formulation by fitting some useful function, such as the hyperbolic sine or a finite power series, to the magnetization curve. On the other hand, a radically different approach exists in which all resemblance to linear behavior of the magnetic material is discarded. (These various analyses of the magnetic amplifier are outlined and compared in reference (8)).

The point to be made is that any refinement of the linear theory which attempts to account for non-linearity leads to very cumbersome mathematical forms. The fresh approach using what might be termed a limiting case for a beginning, may, if carefully applied, lead to a mathematical formulation even simpler than in the linear case. This seems to be true of the method suggested by Ganz. It is the purpose of this paper to show a logical transition from the linear theory of eddy currents in solid media to the method of Ganz, and to show the applicability of the method in typical problems. Two other theories, those of Rosenberg and of Barth, will be included for comparison.

Comparison of Linear and Limiting Non-Linear Theories

The linear theory will be reviewed by the use of a simple situation. An infinite half-space with its surface in the x,y plane is excited such that the total magnetic flux carried in the x direction per unit of width in the y direction is $Re\ \phi_{max} e^{j\omega t}$. There is no y or z component of flux. The z direction extends into the material normal to the x,y plane. The permeability of the material is μ, its conductivity is σ, and the radian frequency is ω. Taking $\overline{B}$, the induction, to be the field variable, the field equations are $B_y = B_z = 0$, and (using MKS units)

$$\frac{\partial^2 B_x}{\partial z^2} = \mu\sigma \frac{\partial B_x}{\partial t} \qquad (1.)$$

The solution is

$$B_x = \mathrm{Re}\ B_o e^{(j\omega t - \sqrt{j\omega\mu\sigma}\, z)} \tag{2}$$

where B_o, a complex number, is the induction at the surface. The total flux per unit width is

$$\phi(t) = \int_o^\infty B_x\, dz = \frac{B_o}{\sqrt{j\omega\mu\sigma}}\, e^{j\omega t} \tag{3}$$

Substituting into (2)

$$B_x = \mathrm{Re}\ \sqrt{j\omega\mu\sigma}\ \phi_{max}\, e^{(j\omega t - \sqrt{j\omega\mu\sigma}\, z)} \tag{4}$$

Expressed in a different form equation (4) becomes

$$B_x = \mathrm{Re}\ \frac{\phi_{max}}{\frac{1}{\sqrt{\omega\mu\sigma}}}\, e^{-\sqrt{\frac{\omega\mu\sigma}{2}}\, z}\ e^{j\left(\omega t + \frac{\pi}{4} - \sqrt{\frac{\omega\mu\sigma}{2}}\, z\right)} \tag{5}$$

where ϕ_{max} is a real number.

The behavior of B_x as a function of time and of depth is illustrated in Figure 1. The upper curve is the total flux $\phi(t)$ while the lower curves give the flux density as a function of time at the various levels. At any instant, the flux density varies as a damped sinusoid with depth; thus there are alternate positively and negatively magnetized bands of material. The existence of these alternate bands can be seen also by inspecting the time function at various levels.

Now the same situation is analyzed once more, but with the linear magnetic material being replaced by a material having the non-linear magnetic characteristic shown in Figure 2. This material is magnetized to saturation if the field intensity is different from zero, and it is possible to change the flux density only at H = 0. The statement implies that if the flux density is changing, H must be zero. However, the converse statement is not necessarily true; if H is zero, the flux density is not necessarily changing. Thus it is possible to have regions within this material where H is zero but where the flux density can have any constant value less than or equal to the saturation induction. The particular constant value would depend upon the state in which the material was left during some previous process.

The mechanics of supporting a function $\phi(t) = \mathrm{Re}\ \phi_{max}\, e^{j\omega t}$ will now be investigated. First it will be assumed that H at any point is a periodic function with fundamental radian frequency ω and no average value. If this function has zeroes only at discrete values of (ωt) which are π radians apart, the corresponding induction B will be a square wave of period $2\pi/\omega$ and amplitude B_s. On the other hand, a square wave of B at any point can be supported by a discontinuous function H (ωt), due to the possibility (discussed above) that B may remain constant when H is zero. Thus it seems reasonable to postulate that the induction at any point in the material is either constant at some value depending on previous treatment or a square-wave with amplitude B_s and period $2\pi/\omega$.

Inspection of Figure 1 gives some insight as to how the square waves giving B as a function of time might combine to give a total flux ϕ (t) which is sinusoidal. In Figure 1, the induction at any level z is a sine wave versus time, but whose phase is shifted with respect to the level above. The next question is, can a succession of square waves which are phase shifted with respect to one another add to a sine wave? Figure 3 shows a finite group of these square waves and their instantaneous sum. (The resemblance to the calculation of the m.m.f. of a distributed winding in a rotating machine is apparent). If there are enough square waves, phase-shifted in a particular manner which can be computed, a smooth sine wave ϕ (t) results.

The computation of this phase shift as a function of depth is better approached by a change of variable. At some instant say $(\omega t)_1$ the induction above the level z_1(Figure 3) is $- B_s$ while below that level it is $+ B_s$. At a later instant $(\omega t)_2$ the induction above the level z_2 has become $-B_s$ while below z_2 it remains $+B_s$. Thus a surface of separation between the two saturated states has moved from z_1 to z_2 during the interval $(t_2 - t_1)$. The phase shift between the square waves of induction at these two levels will be $\omega(t_2 - t_1)$ radians. The distance $(z_2 - z_1)$ that the surface of separation has moved, and the phase shift $\omega(t_2 - t_1)$ radians, are both related to the change in flux per unit width $\Delta\phi$ which has occured during that time.

The surface of separation will stop when there is no further need to "subtract flux" by causing this change to take place. The maximum distance that this surface travels, beginning at $z = 0$, will be the depth of penetration δ. When the surface of separation has reached the depth $z = \delta$, the flux per unit width will be $- \phi_{max}$. The depth of penetration is

$$\delta = \frac{\phi_{max}}{B_s} \tag{6}$$

This movement from $z = 0$ to $z = \delta$ has occurred in a half cycle, since the flux per unit width has been changed from ϕ_{max} to $-\phi_{max}$. Thus, the phase shift between square square waves of B versus (ωt) at $z = 0$ and $z = \delta$ is π radians.

The depth of penetration δ is seen to be a variable depending on ϕ_{max}, while in the linear material the depth of penetration is a property of the material at a given frequency (equation 4). This behavior is expected, since in the linear material it is possible to increase $B_{x\,max}$ if more flux is required; in the nonlinear material the induction is limited to B_s, and more flux can be obtained only if δ increases.

The position of the surface of separation will now be determined as a function of the flux ϕ. Let the location of the surface be z'. The flux per unit width contributed when the surface moves from z' to $(z' + \Delta z')$, changing the state from $+B_s$ to $- B_s$, will be

$$\Delta\phi = -2B_s \Delta z' \tag{7}$$

Passing to the limit $\Delta\phi \to 0$ yields the differential equation for z'

$$\frac{dz'}{d\phi} = -\frac{1}{2B_s} \tag{8}$$

The integration will be performed beginning at the time when $\phi = +\phi_{max}$ and $z' = 0$. (Calculations begun when $\phi = -\phi_{max}$ would proceed in the same way with a change in sign, such that z' is always a positive increasing function.) Thus,

$$z'(\phi) = \frac{1}{2B_s} \int_{\phi_{max}}^{\phi} -d\phi \tag{9}$$

or

$$z'(t) = \frac{\phi_{max} - \phi(t)}{2B_s} \tag{10}$$

The next problem is to compute the phase shift at different depths. The square wave of B versus (ωt) at any level z may be expressed by

$$B(\omega t) = B_s \square(\omega t - \psi) \tag{11}$$

where the symbol " $\square(x)$ " represents a periodic function of x which is a square wave of amplitude 1 and period $(2\pi/\omega)$. The angle ψ is the phase displacement between the origin of the square wave at depth z and the origin of the square wave at z = 0, so ψ will be a function of z. The origin of the square wave is taken at the center of the positive flat portion.

Equation (10) was derived assuming that at time zero, the flux is a positive maximum and is being decreased. Thus, at time zero all the material was previously magnetized to $+B_s$ induction, and will be changed during the subsequent half cycle to $-B_s$ induction. At z = 0 the origin of the square wave would be located at $\psi = -\pi/2$, since at time zero, that value of ($\omega t - \psi$) must be $\pi/2$. The further dependence of ψ upon z can be deduced from Equation (10), since when the surface of separation is located at $z' = z$ we must have ($\omega t - \psi$) = $\pi/2$ at that level. Thus, setting $z'\left(\frac{\pi/2 + \psi}{\omega}\right) = z$:

$$z = \frac{\phi_{max} - \phi\left(\frac{\pi/2 + \psi}{\omega}\right)}{2B_s} \tag{12}$$

If now $\phi = \mathrm{Re}\, \phi_{max} e^{j\omega t}$ is substituted in (12), the relationship between ψ and z for that case is

$$z = \frac{\phi_{max}}{2B_s}\left[1 - \cos\left(\frac{\pi}{2} + \psi\right)\right] = \frac{\delta}{2}\left[1 + \sin\psi\right] \tag{13}$$

or

$$\sin\psi = 2\frac{z}{\delta} - 1 \tag{14}$$

Thus, $\psi(0) = -\pi/2$ and $\psi(\delta) = \pi/2$, signifying that the square waves are phase shifted by a half period over the depth δ. For $z > \delta$, that is, below the depth of penetration, no change in induction occurs.

The results of this computation for B as a function of depth and time are summarized in Figure 4. The same values of ϕ_{max} and ω are used in Figures 1 and 4, while values of μ and σ have been chosen so that the extinction of the field takes place in about the same depth in both cases. The peak value of induction is seen to be much higher in Figure 1 than in Figure 4, while the phase shift is larger in Figure 4. The different phase shift might have been anticipated; in the linear case, Figure 1, the contribution to ϕ (t) by the lower levels, where the phase is advanced, has been reduced due to the damping affect. In the non-linear case this gradual damping does not exist. This comparison also validates the idea of using square waves of flux; the saturation induction is reached very early in the cycle in Figure 1.

An Intermediate Theory

A theory to account for saturation which is in a sense intermediate between the linear theory and the limiting non-linear theory has been proposed by Barth (reference 3). It is assumed that the flux density varies sinusoidally with time at any level, as in the linear theory, but that the amplitude of the sine wave is B_s at every level (except possibly in that part of the material which experiences no change in induction). The differential equations of the field are used as in the linear theory. The field equations become, in MKS units,

$$\begin{cases} \text{curl } \vec{E} = -\dfrac{\partial \vec{B}}{\partial t} \\ \text{curl } \vec{H} = \vec{J} \end{cases} \qquad \begin{cases} \text{div } \vec{B} = 0 \\ \vec{J} = \sigma \vec{E} \end{cases} \tag{15}$$

which reduce to the form

$$\begin{cases} \text{div } \vec{B} = 0 \\ \text{curl curl } \vec{H} = -\sigma \dfrac{\partial \vec{B}}{\partial t} \end{cases} \tag{16}$$

At this point in the linear theory, the relationship $\vec{B} = \mu \vec{H}$ is used, to yield the equations

$$\begin{cases} \text{div } \vec{B} = 0 \\ \text{grad div } \vec{B} - \Delta \vec{B} = -\mu\sigma \dfrac{\partial \vec{B}}{\partial t} \end{cases} \tag{17}$$

which can be reduced to equation (1). However, in the present case, the transition from equation (16) to equation (17) cannot be made. Instead, it is found

$$\begin{cases} \text{div } \vec{B} = 0 \\ \text{grad div } \vec{H} - \Delta \vec{H} = -\sigma \dfrac{\partial \vec{B}}{\partial t} \end{cases} \tag{18}$$

Before proceeding, it is necessary to expand equations (18) and interpret them according to the assumed field distribution.

Again it is assumed that $\overline{B}$ has only and x-component and this component varies only with z. Therefore $div\,\overline{B} = 0$ is automatically satisfied. It is now assumed that $\overline{B}$ and $\overline{H}$ are co-linear vectors, although they bear no linear relationship to one another. Thus $\overline{H}$ has only an x-component. By symmetry, it is assumed that this component varies only with z. In this particular situation, therefore, $div\,\overline{H} = 0$ also. The field equations now reduce to

$$\frac{\partial^2 H_x}{\partial z^2} = \sigma \frac{\partial B_x}{\partial t} \tag{19}$$

It is now assumed that H_x and B_x at any level z are both sinusoidal time functions, and that they are in phase. Thus

$$\begin{cases} H_x = H\, e^{j\psi}\, e^{j\omega t} \\ B_x = B_s\, e^{j\psi}\, e^{j\omega t} \end{cases} \tag{20}$$

where both ψ and H are real functions of z. Substituting into equation (19),

$$\frac{d^2}{dz^2}\left(He^{j\psi}\right) = j\omega\sigma B_s e^{j\psi} \tag{21}$$

(These equations neglect the hysteresis effect, while in Barth's original paper this effect is taken into account by introducing a constant phase difference β between H and B in equation (20).)

On performing the differentiation in equation (21) and equating real and imaginary parts, the following differential equations are obtained:

$$\begin{cases} \ddot{H} - H\dot{\psi}^2 = 0 \\ 2\dot{H}\dot{\psi} + H\ddot{\psi} = \omega\sigma B_s \end{cases} \tag{22}$$

where the dot signifies differentiation with respect to z. By inspection of these equations, Barth concluded that H must be parabolic in the variable (z/z_o) while ψ must be logarithmic in the same variable. The result obtained by Barth is that

$$\begin{cases} H = H_o \left(\frac{z}{z_o}\right)^2 \\ \psi = \sqrt{2}\, \ln\left(\frac{z}{z_o}\right) \\ z_o = \sqrt{\frac{3\sqrt{2}\, H_o}{\omega\sigma B_s}} \end{cases} \tag{23}$$

where the coordinate z is measured from the level z_o, inside the material, positive toward the interface between iron and air. The field intensity applied at the surface is H_o. The flux per unit width turns out to be

$$\phi(t) = B_s \frac{\delta_o}{\sqrt{3}} e^{j(\omega t - \tan^{-1}\sqrt{2})} \tag{24}$$

from which, also,

$$\delta_o = \sqrt{3} \frac{\phi_{max}}{B_s} \tag{25}$$

The Theory of Rosenberg

Rosenberg's treatment (reference 2) assumes that the flux density is a sinusoidal function, without phase shift from layer to layer, and with a constant amplitude B_{max} between z = 0 and z = $\underline{a}$. The amplitude B_{max} and the depth of penetration $\underline{a}$ are related, however, the connecting variable being the field intensity at the surface H_o; in turn, H_o and B_{max} are related through the saturation curve. The two expressions for $\underline{a}$ corresponding to equations (23) and (25) for z_o are (in MKS units)

$$\begin{cases} a = \sqrt{\dfrac{2H_o}{\omega\sigma B_{max}}} \\ a = \phi_{max}/B_{max} \end{cases} \tag{26}$$

When ϕ_{max} is given and it is required to find B_{max}, H_o and $\underline{a}$, the computation is based upon the elimination of $\underline{a}$ in equations (26):

$$\phi_{max} = \sqrt{\frac{2H_o B_{max}}{\omega\sigma}} \tag{27}$$

The saturation curve relates B_{max} to H_o. With ω and σ fixed, ϕ_{max} may be plotted versus H_o. Thus H_o and B_{max} may be found, and either of equations (26) determines $\underline{a}$.

Rosenberg noted in the original paper that the two most prominent assumptions, that is, that the amplitude of the flux density is constant and that the phase shift from layer to layer is negligible, introduce compensating errors in the computation of eddy current loss. Barth found that the inclusion of phase shift but the omission of time harmonics yields about the same results as the Rosenberg treatment. It will be shown that the Ganz treatment, which takes both these effects into account, yields higher losses.

Eddy Currents According to the Treatment of Ganz

A basic assumption in Ganz's treatment is that a change in induction can take place only when H = 0. Therefore, the sum of all the field intensities at the surface of separation between the states $-B_s$ and $+B_s$ must be

zero. This statement allows the derivation of a relationship among the flux, the externally applied field, and the eddy currents.

The field equations which relate the density of eddy currents to the rate of change of magnetic induction are

$$\begin{cases} \vec{J} = \sigma \vec{E} \\ \text{curl } \vec{E} = -\dfrac{\partial \vec{B}}{\partial t} \end{cases} \tag{28}$$

The second of equations (28) says that the electric field intensity $\vec{E}$ is everywhere irrotational, because the induction can be only $\pm \vec{i} B_s$ where $\vec{i}$ is the unit vector in the x-direction. The only possible irrotational vector $\vec{E}$ under the conditions set for the problem is a vector varying in time but not varying with position at a given instant. To find out what $\vec{E}$ is, it is necessary to convert the second of equations (28) to the integral form, yielding

$$\begin{cases} \vec{J} = \sigma \vec{E} \\ \oint_C \vec{E} \cdot d\vec{r} = -\dfrac{\partial}{\partial t} \iint_S \vec{B} \cdot d\vec{S} \end{cases} \tag{29}$$

where C bounds $\vec{S}$ and traverses $\vec{S}$ in the usual counter-clockwise sense.

The line integral in equations (29) will be zero if C lies entirely on one side of the surface of separation between $-B_s$ and $+B_s$. However, if C cuts this surface, then the integral over $\vec{S}$ will have a time derivative depending upon the velocity of the surface of separation and the length of the segment common to both $\vec{S}$ and the moving surface. Thus a discontinuity in $\vec{E}$ is expected at the moving surface.

The integrals in equations (29) are easily evaluated in the particular example being considered. Since $\vec{B}$ has only an x-component, the surface $\vec{S}$ is taken in the y,z plane. The surface of separation between states $-B_s$ and $+B_s$ is an x,y plane moving in the z-direction. The segment common to both these surfaces will be Δ y meters long. The electric field $\vec{E}$ will have a y-component only, which will (at any instant) take constant values above and below the surface of separation, with a discontinuity at the surface. The situation is illustrated in Figure 5.

Let the induction (in the x-direction) be $-B_s$ above the surface and $+B_s$ below, with the surface moving at velocity (dz'/dt) meters/sec. At time t, let $\vec{S}$ have S_1 area in the region of $-B_s$ induction and S_2 area in the region of $+B_s$ induction. At time $(t + \Delta t)$ the surface will have moved a distance $(dz'/dt)\cdot(\Delta t)$ meters, so that now there will be $[S_1 + (dz'/dt)(\Delta t)(\Delta y)]$ area in the region of $-B_s$ induction and $[S_2 - (dz'/dt)(\Delta t)(\Delta y)]$ area in the region of $+B_s$ induction. The integration in equations (29) becomes

$$\left[E_y\Big|_{z'-\Delta z}\right](\Delta y) - \left[E_y\Big|_{z'+\Delta z}\right](\Delta y) = \frac{2B_s(dz'/dt)(\Delta t)(\Delta y)}{\Delta t} \tag{30}$$

or

$$E_y\Big|_{z'-\Delta z} - E_y\Big|_{z'+\Delta z} = 2B_s \frac{dz'}{dt} \tag{31}$$

Equation (31) gives the discontinuity in the electric field existing at the moving surface separating $-B_s$ and $+B_s$.

There can be no electric field below the moving surface, for if it were to exist, energy would be required to sustain the resulting eddy currents, and there is no such energy available. Therefore,

$$\begin{cases} E_y = 2B_s \dfrac{dz'}{dt} & (0 \leq z < z'); \left(B_x\Big|_{z'-\Delta z} = -B_s\right) \\ E_y = 0 & (z' \leq z) \end{cases} \tag{32}$$

During the succeeding half cycle, E_y reverses sign, since in that interval the induction is being changed from $-B_s$ to $+B_s$ and (dz'/dt) remains positive.

The eddy currents flow with uniform density (at any instant) in the space ($0 \leq z < z'$) and there are no eddy currents below the level z'. The total current contained in the eddy current paths is, by equations (28) and (32)

$$I_e = 2B_s \sigma z' \frac{dz'}{dt} \quad \text{amp/meter} \tag{33}$$

during the half cycle in which the material is being changed from $+B_s$ to $-B_s$. During the following half-cycle, I_e changes sign. Since the field intensity must be zero at the surface between $-B_s$ and $+B_s$, the applied field intensity must be the opposite of equation (33); in other words, the applied field must be $-I_e$ amperes per meter.

An expression for the applied field J_s can be obtained from equations (33) and (10); that is, for sinusoidal flux variation,

$$J_s = -2B_s\sigma\left(\frac{\phi_{max}-\phi(t)}{2B_s}\right)\left(-\frac{1}{2B_s}\frac{d\phi}{dt}\right) = \frac{\sigma}{2B_s}(\phi_{max}-\phi)\frac{d\phi}{dt} \tag{34}$$

In the present case, $\phi = \phi_{max}\cos(\omega t)$ so that during the half cycle when ϕ proceeds from $+\phi_{max}$ to $-\phi_{max}$

$$J_s = -\frac{\omega\sigma}{2B_s}\phi_{max}^2(1-\cos\omega t)\sin\omega t \quad \text{amp/meter} \tag{35}$$

Equation (35 is similar to Equation (9) of reference 6. The wave form of J_s is repeated during the following half cycle but with reversed sign (it is convenient to establish a new time origin each half cycle).

Historical Development of the Non-Linear Treatment

Rosenberg's treatment of eddy current loss in solid iron was the first attempt of practical value to account for the effect of saturation. It was based on an hypothesis which fitted quite well with the overall test results then known. However, the essential nature of the field problem was not considered, since Rosenberg neglected both the phase shift in the field from layer to layer and the fact that the induction at any depth must have prominent time harmonics. Barth made the next step by removing one of these assumptions; his work took the phase shift into account but still neglected the effect of time harmonics. As a result both Rosenberg's and Barth's treatments yield a sinusoidal flux for a sinusoidal current, which is known to be in error, especially when core materials are used whose characteristics approach Figure 2. It has been shown here that the Ganz treatment takes into account both the phase shift and the time harmonics. The test results reported by Hale and Richardson (reference 6) confirm its validity.

Applications of the Ganz Treatment

Applications of this new theory have been restricted so far to the computation of eddy-current loss in thin sheets (reference 6) and the explanation of certain effects in pulse transformer cores (reference 7). To illustrate the versatility of the theory, it will be used in two other problems of continuing interest. These are the computation of losses in solid iron conductors, and the design of inductive heating apparatus for use on a charge of solid iron.

Losses in Iron Wire

The first problem is to deduce the field configuration within the wire under the assumptions used by Ganz. The current will flow in the axial direction, and the wire will become magnetized in a circumferential sense. Suppose for the moment that a steady direct current flows in the wire. The current density will be uniform, and application of Ampere's law shows that H has a value everywhere within the wire, being zero at the center only. According to the assumed magnetic characteristic, the induction will be B_s everywhere within the wire, directed circumferentially. Now if the direct current is reduced to zero the wire will remain in this magnetic state.

Next suppose that a direct current of opposite sign is to be established. The new steady magnetic state will be at saturation induction, but in the opposite direction. The change in induction can occur only if H = 0. Ampere's law leads to the conclusion that there must be a circular region within the wire which carries no current, such that H = 0 at the boundary of this region; the induction is the old value of (say) $- B_s$ in that region. The new current to be established is forced to flow outside this region. As the new current builds up, the region of $- B_s$ is forced to shrink toward the center, and after a time complete reversal of the induction within the wire may be accomplished.

Figure 6 shows the wire, with the boundary between state $+B_s$ and

$-B_s$ located at $r = r'$. This moving boundary causes a change in the flux-linkage with that part of the wire within the boundary, that is, $r < r'$, while the part of the wire in the region $r' < r < R$ sees no change in flux linkage (except the change in the field outside the wire, which is common to both regions and need not be considered). Since the axial electric field is the same in both regions, the resistance drop in the region carrying current can be equated to the drop due to induced e.m.f. in the region carrying no current.

Right-handed cylindrical coordinates are used (Figure 6). At time t, the surface of separation is located at $r = r'$. The electric field in volts per meter, E_z, impressed along the element whose area is dS is to be computed. The flux linkage with that section at time t is

$$\lambda(t) = -B_s (r' - r_s) + B_s (R - r') \quad \text{webers/meter} \qquad (36)$$

At time $(t + \Delta t)$, the surface has moved to $(r' + \Delta r')$ and the flux linkage has changed to

$$\lambda(t+\Delta t) = -B_s[(r'+\Delta r') - r_s] + B_s[R - (r'+\Delta r')] \quad \text{webers/meter} \qquad (37)$$

On passing to the limit, it is found that

$$\frac{d\lambda}{dt} = -2B_s \frac{dr'}{dt} \qquad (38)$$

which is independent of r_s. Therefore every element dS within the region $0 < r < r'$ sees the same electric field impressed, which is

$$E_z = -2B_s \frac{dr'}{dt} \qquad (0 \leq r < r') \qquad (39)$$

Outside this region the electric field E_z is used up in ohmic drop only. (Consequently there is no reactive voltage due to partial flux linkages within this type of conductor).

The current density in the conducting annulus is

$$J = -\sigma \cdot 2B_s \frac{dr'}{dt} \qquad (r' < r \leq R) \qquad (40)$$

The total current being carried by the wire is

$$i = \pi J (R^2 - r'^2) \qquad (41)$$

or

$$i(t) = -2B_s \pi \sigma \left(R^2 - r'^2 \right) \frac{dr'}{dt} \tag{42}$$

which can be integrated to find the coordinate r' as a function of time:

$$\int_R^{r'} -2\pi B_s \sigma (R^2 - r'^2)\, dr' = \int_o^t i(t)dt \tag{43}$$

The situation shown in Figure 6 calls for i(t) to be positive, since the induction is being changed to $+B_s$. If for example i(t) is a sinusoidal function, then equation (43) would become $(0 \leq \omega t \leq \pi)$

$$\frac{2}{3}\pi B_s \sigma \left[r'^3 - 3R^2 r' + 2R^3 \right] = \frac{I_{max}}{\omega} (1 - \cos \omega t) \tag{44}$$

Three situations can be recognized in equation (44). First, the maximum current might not be sufficient to cause the surface of separation to move all the way to the center. An equivalent effect is caused by an increase in frequency. Under such conditions, the depth of penetration will be

$$\begin{cases} \delta = R - r'_{min} \\ \delta < R \end{cases} \tag{45}$$

which can be computed from equation (44) as

$$\frac{2}{3}\pi B_s \sigma \delta^2 (3R - \delta) = \frac{2 I_{max}}{\omega} \tag{46}$$

If now there is pronounced skin effect, that is $\delta << R$, the depth of penetration is

$$\delta \cong \sqrt{\frac{I_{max}}{\pi R B_s \omega \sigma}} \tag{47}$$

which expressed in terms of the maximum apparent surface current density, $J_{smax} = (I_{max}/2\pi R)$ amperes per meter, is

$$\delta \cong \sqrt{\frac{2 J_{smax}}{\omega \sigma B_s}} \tag{48}$$

The second situation which may be identified in equation (44) is that the current and frequency might be such that the surface of separation just reaches the center (r' = 0) at the end of a half cycle. The current

necessary to cause this condition is found from equation (44):

$$I_{max} = \frac{2}{3}\pi\omega\sigma B_s R^3 \quad \text{amperes} \tag{49}$$

The third situation occurs if the current is so large that r' becomes zero before the end of the half cycle; if so, the wire exhibits a constant resistance for the remainder of the half cycle, equal to its d-c resistance.

The effective resistance may be computed for the case of pronounced skin effect ($\delta << R$). The loss density as a function of time will be in general (from equation 41)

$$p(t) = \frac{J^2}{\sigma} = \frac{i^2(t)}{\pi^2\sigma\,(R^2 - r'^2)^2} \quad \text{watts/meter}^3 \tag{50}$$

and the loss per meter of length will be

$$P(t) = \frac{i^2(t)}{\pi\sigma\,(R^2 - r'^2)} \quad \text{watts/meter} \tag{51}$$

in which r' is a function of time which can be deduced from equation (43). The result is

$$P(t) \cong \sqrt{\frac{B_s}{2\pi R\sigma}}\ \frac{i^2(t)}{\sqrt{\int_0^t i(t)dt}} \quad \text{watts/meter} \tag{52}$$

If the current is a sinusoidal function,

$$P(t) \cong I_{max}^{3/2}\sqrt{\frac{B_s\omega}{2\pi R\sigma}}\left[\frac{\sin^2\omega t}{\sqrt{1-\cos\omega t}}\right] \quad \text{watts/meter} \tag{53}$$

The average power dissipated in heat over the half cycle will be

$$P_{av} \cong I_{max}^{3/2}\sqrt{\frac{B_s\omega}{2\pi R\sigma}} \cdot \frac{1}{\pi}\int_0^{\pi}\frac{\sin^2\theta}{\sqrt{1-\cos\theta}}\,d\theta \tag{54}$$

or

$$P_{av} \cong I_{max}^{3/2}\sqrt{\frac{B_s\omega}{2\pi R\sigma}} \cdot \frac{4\sqrt{2}}{3\pi} \quad \text{watts/meter} \tag{55}$$

When this power is expressed in terms of the depth of penetration, as computed from equation (47), it becomes

$$P_{av} \cong I_{max}^2 \cdot \frac{8}{3\pi} \cdot \frac{1}{2\pi R\delta\sigma} \quad \text{watts/meter} \tag{56}$$

The effective resistance of the iron wire is defined by the expression $P_{av} = I^2_{rms} R_{eff}$, yielding

$$R_{eff} = \frac{16}{3\pi}\left(\frac{1}{2\pi R \delta \sigma}\right) \quad \text{ohms/meter} \qquad (57)$$

A conductor whose corss section is not circular, such as a rail, can be treated according to formula (57) if the perimeter of the cross section is substituted for the quantity $2\pi R$.

The depth of penetration (equation 48) is identical with that given by Rosenberg. It must be recognized, however, that there is a basic difference between the field models assumed by Rosenberg and by Ganz. This difference leads to higher losses computed according to the Ganz treatment, as will be shown in equation (59). These similarities and differences will now be examined.

Rosenberg assumes that the current density, at any instant, is a maximum at the surface of the conductor and decreases at a uniform rate with depth, becoming zero at depth δ. Further, the current density at any level is in time phase with the current density everywhere else. Thus the depth of penetration and the depthwise average current density are related according to

$$I_{max} = 2\pi R \delta J_{max} \qquad (58)$$

while the actual maximum current density, at the surface of the conductor, is $2 J_{max}$.

According to the Ganz treatment, there is an annular region at any instant in which the current density is uniform while the rest of the conductor carries no current. The thickness of this annulus varies with time and the current density within the annulus varies with time also (equations 43 and 40). However, when the annulus is thickest, the current is maximum, and the current density at that instant is the same as the average given by Rosenberg (equation 58). Thus it is expected that the Ganz and Rosenberg theories should give the same depth of penetration.

The ratio of loss per meter computed by Rosenberg to that computed according to the Ganz treatment is

$$\frac{P_R}{P_G} = \left[\frac{2}{3}\,\frac{I^2_{max}}{(2\pi R)\delta\sigma}\right] \Big/ \left[\frac{8}{3\pi}\,\frac{I^2_{max}}{(2\pi R)\delta\sigma}\right] \qquad (59)$$

or, the Ganz treatment yields $(4/\pi) = 1.273$ times as much loss as Rosenberg's theory in the case of iron conductors with pronounced skin effect. The increased loss is attributed to the combined effect of phase shift within the field and the presence of time harmonics, both of which were neglected by Rosenberg.

Inductive Heating of Iron in Single-Phase Fields

The relationship between the surface field intensity and the total eddy current given by equation (33) for a plane configuration may be used for the treatment of inductive heating effects if the least dimension of the surface to be heated is much greater than the depth of penetration. For example, if the applied field intensity is a sinusoidal function, equation (33) becomes

$$2B_s\sigma\, z' \frac{dz'}{dt} = J_{smax} \sin \omega t \qquad (60)$$

for each half cycle. The location of the surface of separation between states $-B_s$ and $+B_s$ is

$$z' = \sqrt{\frac{1}{B_s\sigma}\int_0^t J_{smax} \sin\omega t\, dt} \qquad \left(0 \leq t \leq \frac{\pi}{\omega}\right) \qquad (61)$$

and the depth of penetration is

$$z'_{max} = \delta = \sqrt{\frac{2 J_{smax}}{B_s \omega \sigma}} \quad \text{meter} \qquad (62)$$

which is equivalent to equation (48).

The current density in the conducting layer will be

$$J = \frac{J_s}{z'} = \sqrt{B_s \omega \sigma J_{smax}}\ \frac{\sin \omega t}{\sqrt{1-\cos \omega t}} \quad \text{amp/meter}^2 \qquad (63)$$

and the loss per square meter of surface area is

$$P = z' \frac{J^2}{\sigma} = J_{smax}^{3/2} \sqrt{\frac{B_s \omega}{\sigma}} \left(\frac{\sin^2 \omega t}{\sqrt{1-\cos \omega t}}\right) \quad \text{watts/meter}^2 \qquad (64)$$

The average loss is

$$P_{av} = \frac{4\sqrt{2}}{3\pi} J_{smax}^{3/2} \sqrt{\frac{B_s \omega}{\sigma}} \quad \text{watts/meter}^2 \qquad (65)$$

which is the equivalent of equation (55). Thus for sinusoidal currents, the conductive and inductive heating processes are identical within the iron, and the same loss formula applies. This fact has been noted by Thornton (section 3.1 of reference 9).

Practical design of an inductive heating installation requires a means to compute the terminal voltage of the exciting winding. The real part of this voltage (in phase with the exciting current) will supply the resistive drop in the exciting circuit plus the equivalent resistance drop induced by the eddy current losses. The reactive part will consist of the reactive drop

induced by the eddy currents plus the reactive drop due to stray magnetic fields (for example, the field existing in the space between the exciting winding and the surface to be heated). The real and reactive parts of the voltage induced by eddy currents will be computed next. The other components of terminal voltage may be computed by well-known methods.

The electric field induced in the exciting current sheet due to flux within the iron is given by equation (32), which when combined with equation (61) yields

$$E = \sqrt{\frac{B_s \omega J_{smax}}{\sigma}} \left(\frac{\sin \omega t}{\sqrt{1-\cos \omega t}} \right) \qquad (0 \le t \le \pi/\omega) \tag{66}$$

which reduces to

$$E = \sqrt{\frac{2 B_s \omega J_{smax}}{\sigma}} \left(\cos \frac{\omega t}{2} \right) \qquad \text{volts/meter} \tag{67}$$

By Fourier analysis, the fundamental component is found to be

$$E_{fund} = \sqrt{\frac{2 B_s \omega J_{smax}}{\sigma}} \left[\frac{8}{3\pi} \sin \omega t + \frac{4}{3\pi} \cos \omega t \right] \tag{68}$$

The phase angle between the electric field and the exciting current is

$$\begin{cases} \theta = \tan^{-1} 0.5 = 26.6^\circ \\ \cos\theta = 2/\sqrt{5} = 0.895 \end{cases} \tag{69}$$

If there are N turns in the exciting coil, each of length U meters, distributed over an axial length ℓ meters, the formula relating voltage and current (exclusive of voltages due to external ohmic drop and stray fields linking the exciting circuit) is

$$V = 2.83 \frac{N^{3/2} U}{\ell^{1/2}} \sqrt{B_s f \rho I} \qquad \text{volts} \tag{70}$$

where V is the rms of the fundamental voltage, I is the rms of the sinusoidal exciting current, f is the frequency in cycles/sec. and ρ ($= 1/\sigma$) is the resistivity of the iron in ohm-meters. The power delivered to the iron is

$$P = 2.53 \frac{N^{3/2} U I^{3/2}}{\ell^{1/2}} \sqrt{B_s f \rho} \qquad \text{watts} \tag{71}$$

The new theory provides a means for computing the power factor of the load reflected into the exciting winding by the eddy currents. Such a computation was not possible using the Rosenberg treatment, since the effect of phase shifts within the field were not taken into account. The power factor of the eddy-current load is seen to be quite high. The relatively

low power factor encountered in inductive heating installations is due to the reactive voltage of the unavoidably large stray magnetic fields.

The wave form of induced e.m.f. as given by equation (67) has been checked experimentally, with the results being presented in Figure 7 and Table 1. Sinusoidal current was forced by connecting an adequate resistance in series with the exciting coil. The sinusoidal current trace is included for phase comparison, and its calibration varies among the different oscillograms. The voltage calibration is the same for all.

The specimen tested was a closed ring of square cross section, 0.5 inch by 0.5 inch, with mean diameter 5.375 inches, made of a particular grade of cast iron having good uniformity and high carbon content. Accordingly, the saturation induction is quite low and the resistivity is high being 0.68 microhm-meter. Magnetic data are given in Table 2. The ring was covered with two layers of ordinary black friction tape and then closely wound with 143 turns of AWG-10 enamel covered copper wire. A search coil of 12 turns was placed outside the exciting winding. Tests were made at 60 cycles.

The oscillograms show the characteristic sharp rise in voltage at the beginning of each half cycle, and gradual decay, as given by equation (67). Furthermore, they show the distinctive behavior expected when the depth of penetration δ becomes approximately equal to, or greater than, half the thickness of the ring. The induced e.m.f. is sharply reduced to a small value and remains there until the magnetic process starts again at the beginning of the next half cycle, the peak voltage at the beginning of the half cycle being unaffected by the later complete magnetic re-orientation of the ring.

The peak to peak search coil voltage has been computed according to equation (67), further modified by Rosenberg's suggestion for determining B_s as discussed under "Additional Remarks" below. The depth of penetration δ has been computed according to equation (62) using the same modification. These results, together with the measured search coil voltage, are presented in Figure 8. The oscillograms show the characteristics of over-excitation at about 20 amperes exciting current, while the dpeth of penetration becomes equal to half the thickness of the ring at 24 amperes. (It should be noted again here that all computations are based upon the assumptions of an infinite plane configuration).

Additional Remarks

A very detailed set of experiments has been reported recently by Thornton (reference 9), in which the losses in mild steel pipe were determined as a function of frequency and of current. The objective of the experiments was to present an empirical method of design for conductive and inductive heating of iron vessels and pipes. It was found that the loss at constant frequency varied as the 1.57 power of the current while the Ganz theory predicts an exponent of 1.50.

A somewhat empirical way of determining B_s, originally proposed by Rosenberg, does in fact lead to a loss exponent for this type of steel which is as near 1.57 as the accuracy of available information allows.

Rosenberg proposed that the value of B_s to be used in a given problem should correspond to the maximum current carried per unit periphery of the conductor (equations 26 and 27). If the magnetization curve for hot-rolled steel sheets (structural or "mild" steel) as given in handbooks is used in this way to compute the loss exponent, excellent agreement with Thorntons value is obtained. However, the agreement extends only over Thornton's range of test information which begins at about 7 oersteds, already well into the region where the induction ceases to change rapidly with applied field.

This empirical method of assigning B_s may be justified somewhat by inspection of equation (55). It is seen that the loss varies as the square root of B_s. The induction increases only moderately with increasing applied field when appreciable saturation is present, and the theory does not apply in the case of small saturation. In view of the small changes in B_s to be expected, and the further appearance of B_s under the radical, the method for taking the variation of B_s into account is not critical. Thus the correlation between B_s and field intensity as obtained from the saturation curve could be expected to yield reasonably good results. In substantiation, the mechanics of the Ganz theory shows that the maximum field intensity is just equal to the maximum amperes per unit of periphery, so that higher values of induction than that taken from the saturation curve would not be expected.

Conclusions

It has been shown that the theory of alternating fields in solid iron proposed by Ganz is a significant advance, in that the objections to Rosenberg's treatment are overcome. Furthermore, a logical transistion from the classical theory to the theory of Ganz has been demonstrated. The losses computed according to the new theory are somewhat higher than those predicted by Rosenberg, as would be expected since the new theory accounts for both time harmonics of current density and phase shifts in the magnetic field. Formulae have been presented which show the usefulness of the new theory as a design method for inductive and conductive heating installations.

Table 1

Oscillograms of Figure 7

Oscillogram	Exciting Current, rms	Search coil volts peak to peak
1 (upper left)	2.5	0.61
2	5.0	1.00
3	7.5	1.31
4	10.0	1.58
5	15.0	1.97
6 (lower left)	20.0	2.30
7 (upper right)	25.0	2.54
8	30.0	2.76
9	35.0	2.97
10	40.0	3.06
11	45.0	3.27
12 (lower right)	50.0	3.30

Table 2

Magnetization Curve of Cast Iron Ring, by Flux-meter

H, amp/meter	B, weber/sq. meter
0	0
1000	0.55
2000	0.76
3000	0.85
4000	0.90
6000	0.97
8000	1.01
10000	1.04
12000	1.05

References

1. R. Rudenberg, "Losses of Eddy Currents in Electric Brakes and Dynamos", Sammlung Elektrotechnischer Vortrage (Stuttgart, Germany) Volume X, 1906, pages 269-370.

2. E. Rosenberg, "Solid Iron Conductors and Eddy Current Brakes", Elektrotechnik and Maschinenbau (Vienna, Austria) volume 41, No. 49, 1923, pages 701-717.

3. J. B. Barth, "Alternating Fields and Eddy Currents in Solid Iron with High Magnetic Saturation", Electrotechnick Tidsskrift (Oslo, Norway), Volume 48, No. 7, 1935, pages 85-99.

4. R. Pohl, "Rise of Flux Due to Impact Excitation: Retardation by Eddy Currents in Solid Parts", Proceedings, Institution of Electrical Engineers, Volume 96, Part 2, 1949, pages 57-65.

5. S. Ya. Dunaevskii, "Influence of Eddy Currents on the Process of Flux Establishment", Elektrichestvo, No. 2 (February, 1951), pages 55-63.

6. J. W. Hale and F. R. Richardson, "Mathematical Description of Core Losses", to be published in the Transactions of the American Institute of Electrical Engineers, Volume 72 (1953).

7. A. G. Ganz, "Application of Thin Permalloy Tape in Wide-Band Telephone and Pulse Transformers", Transactions American Institute of Electrical Engineers, Volume 65 (1946), pages 177-183.

8. L. A. Finzi and G. F. Pittman, Jr., "Comparison of Methods of Analysis of Magnetic Amplifiers", Proceedings of the National Electronics Conference, Volume 8, January 1953, pages 144-157.

9. C.A.M. Thornton, "Resistance Heating of Mild-Steel Containers at Power Frequencies", Proceedings of the Institute of Electrical Engineers, Vol. 99 Part 2 (1952), pages 85-93.

CAPTIONS FOR FIGURES

Figure 1. Flux per unit width and flux density in the classical theory with constant permeability.

Figure 2. Assumed magnetic characteristic.

Figure 3. Arrangement of square waves adding to a smooth periodical function.

Figure 4. Sinusoidal flux per unit width in saturated solid ion and square waves of flux density at various depths.

Figure 5. Definition of symbols used in the plane configuration.

Figure 6. Definition of symbols used in the cylindrical configuration.

Figure 7. Induced e.m.f. of a search coil wound on a solid iron ring excited with sinusoidal current.

Figure 8. Computed and measured search coil voltage.

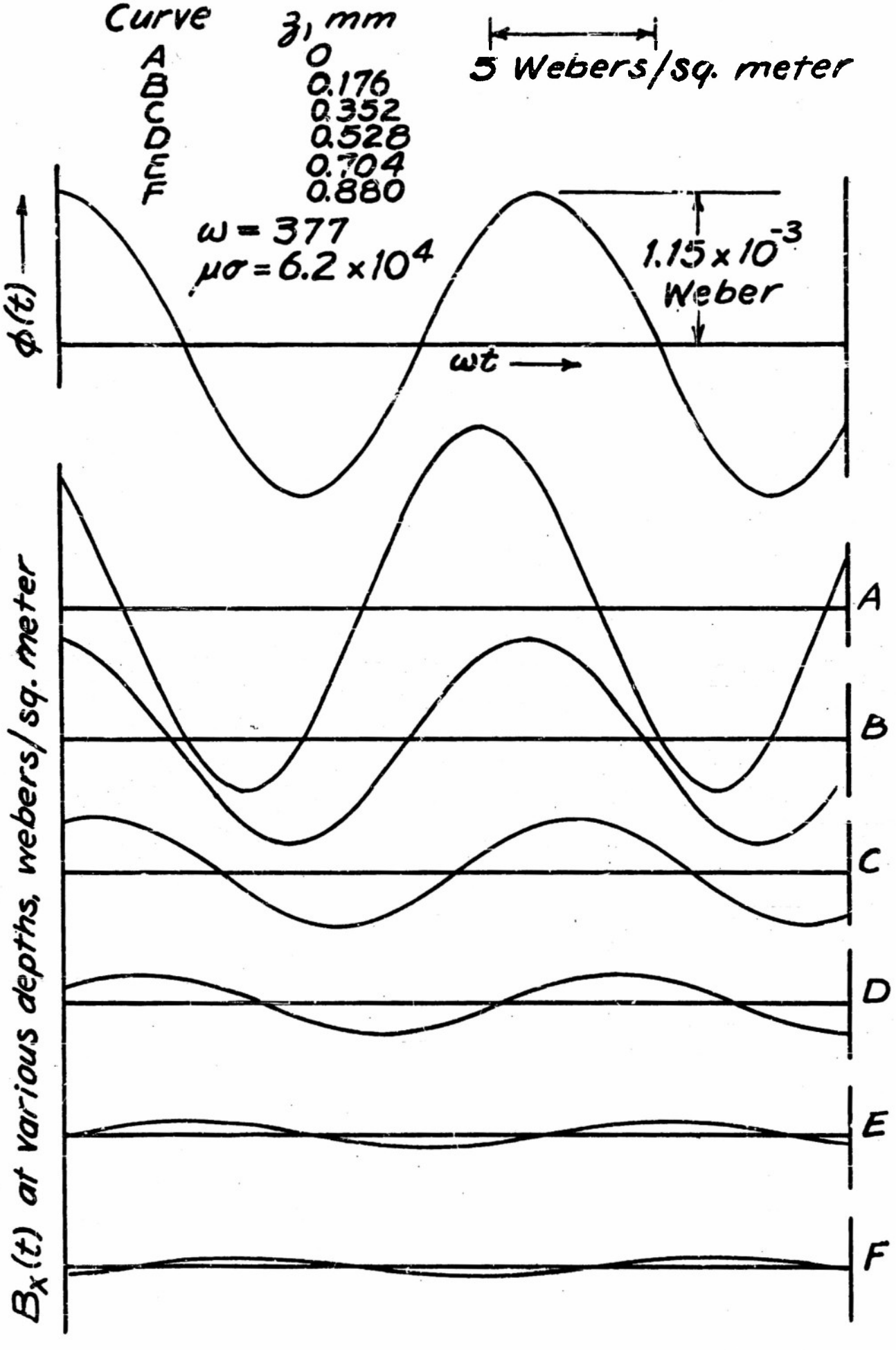
Curve
z, mm
A 0
B 0.176
C 0.352
D 0.528
E 0.704
F 0.880
5 Webers/sq. meter
ω = 377
μσ = 6.2 × 10^4
1.15 × 10^-3 Weber
φ(t)
ωt
A
B
C
D
E
F
Bx(t) at various depths, webers/sq. meter

Figure 1

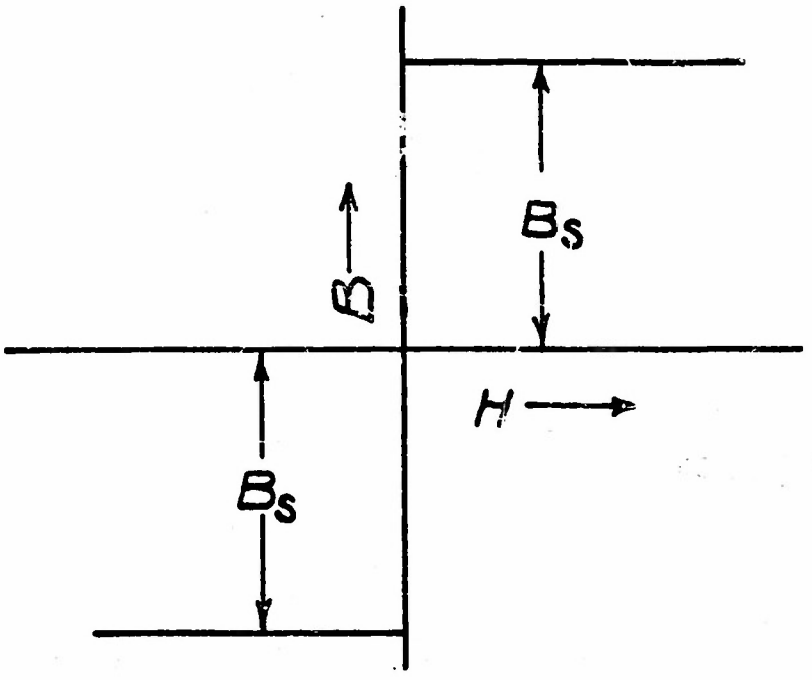

Figure 2

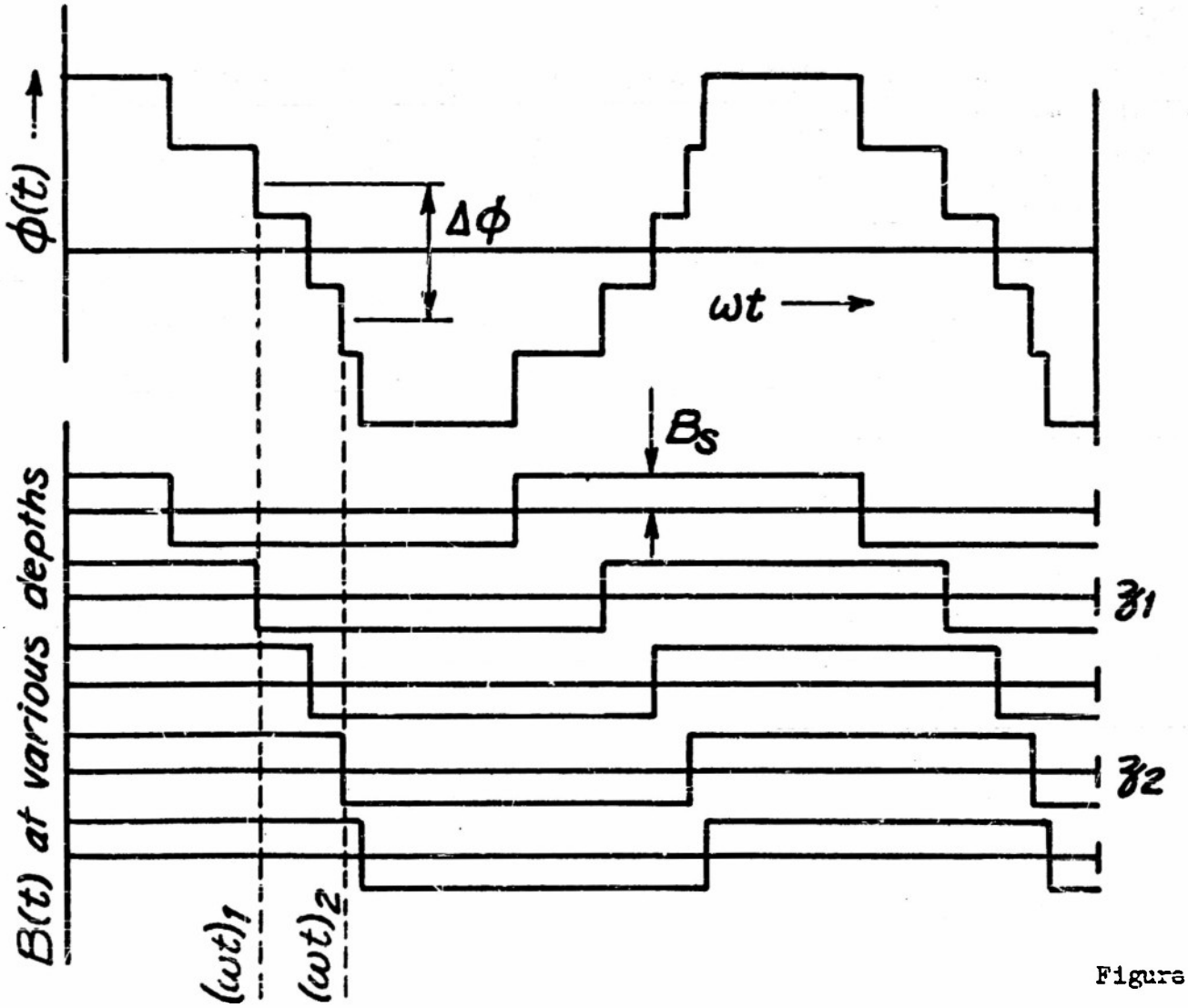

Figure 3

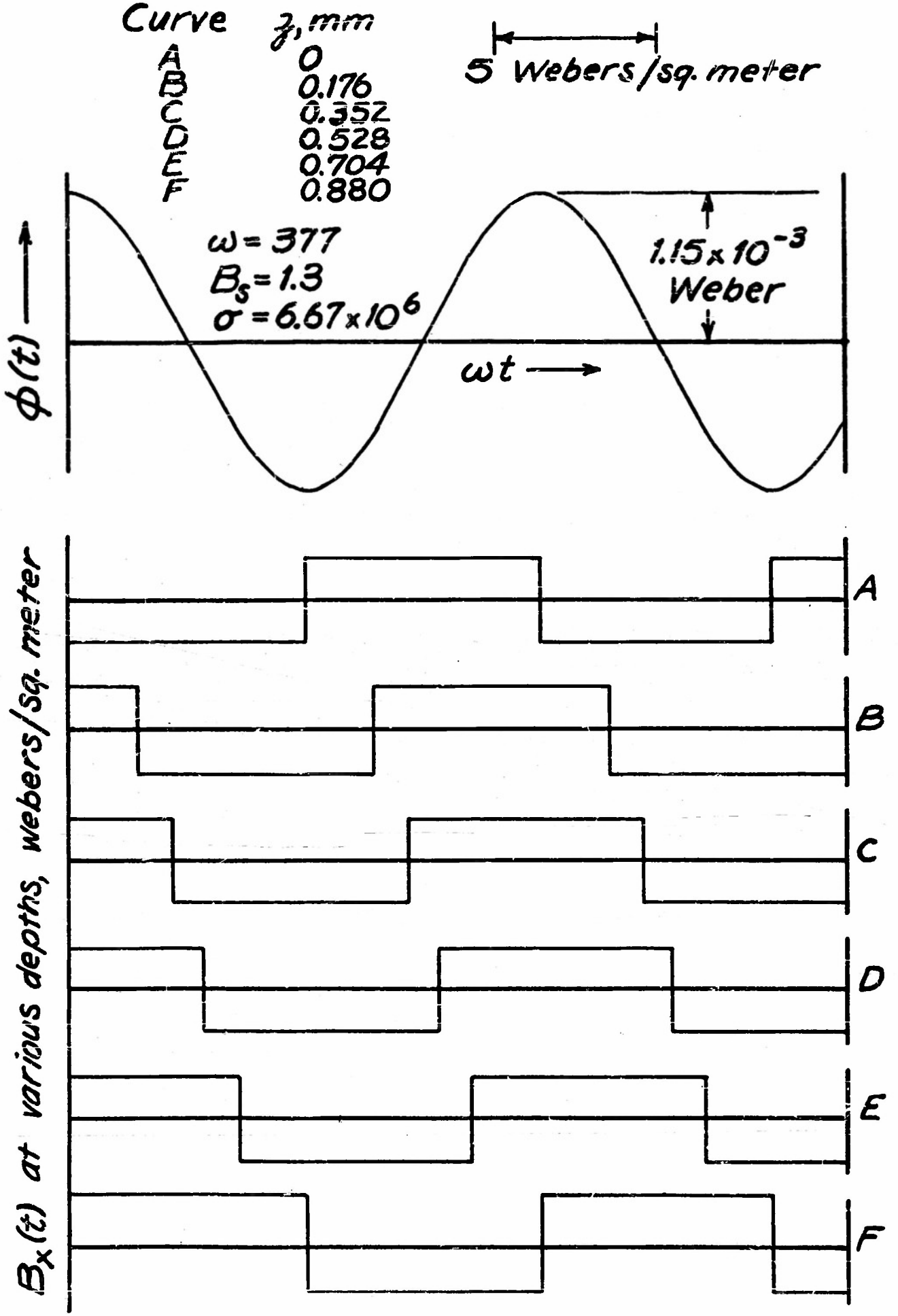
Curve
z, mm
A 0
B 0.176
C 0.352
D 0.528
E 0.704
F 0.880
5 Webers/sq. meter
ω = 377
B_s = 1.3
σ = 6.67 x 10^6
1.15 x 10^-3 Weber
φ(t)
ωt
$B_x(t)$ at various depths, webers/sq. meter
A
B
C
D
E
F

Figure 4

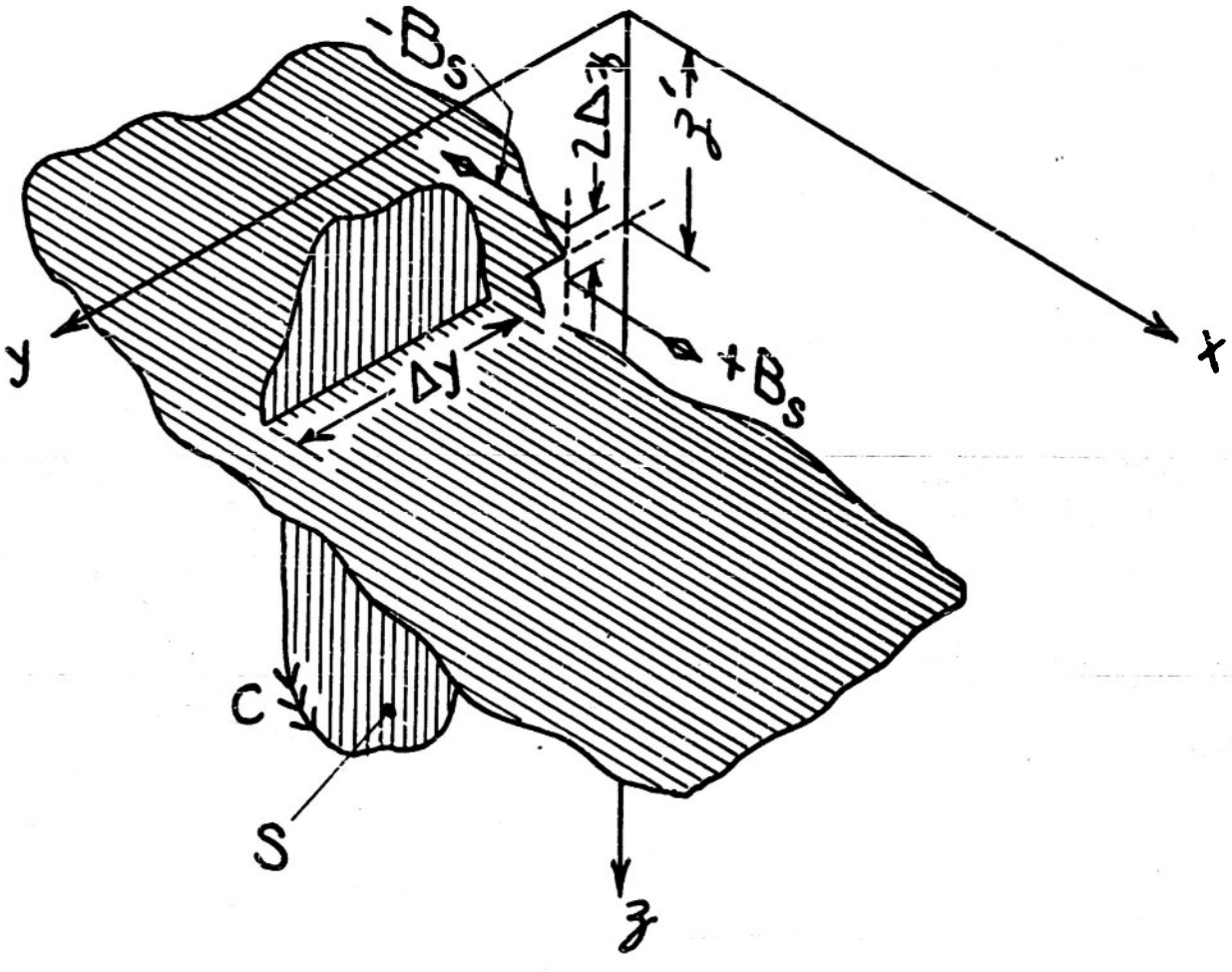

Figure 5

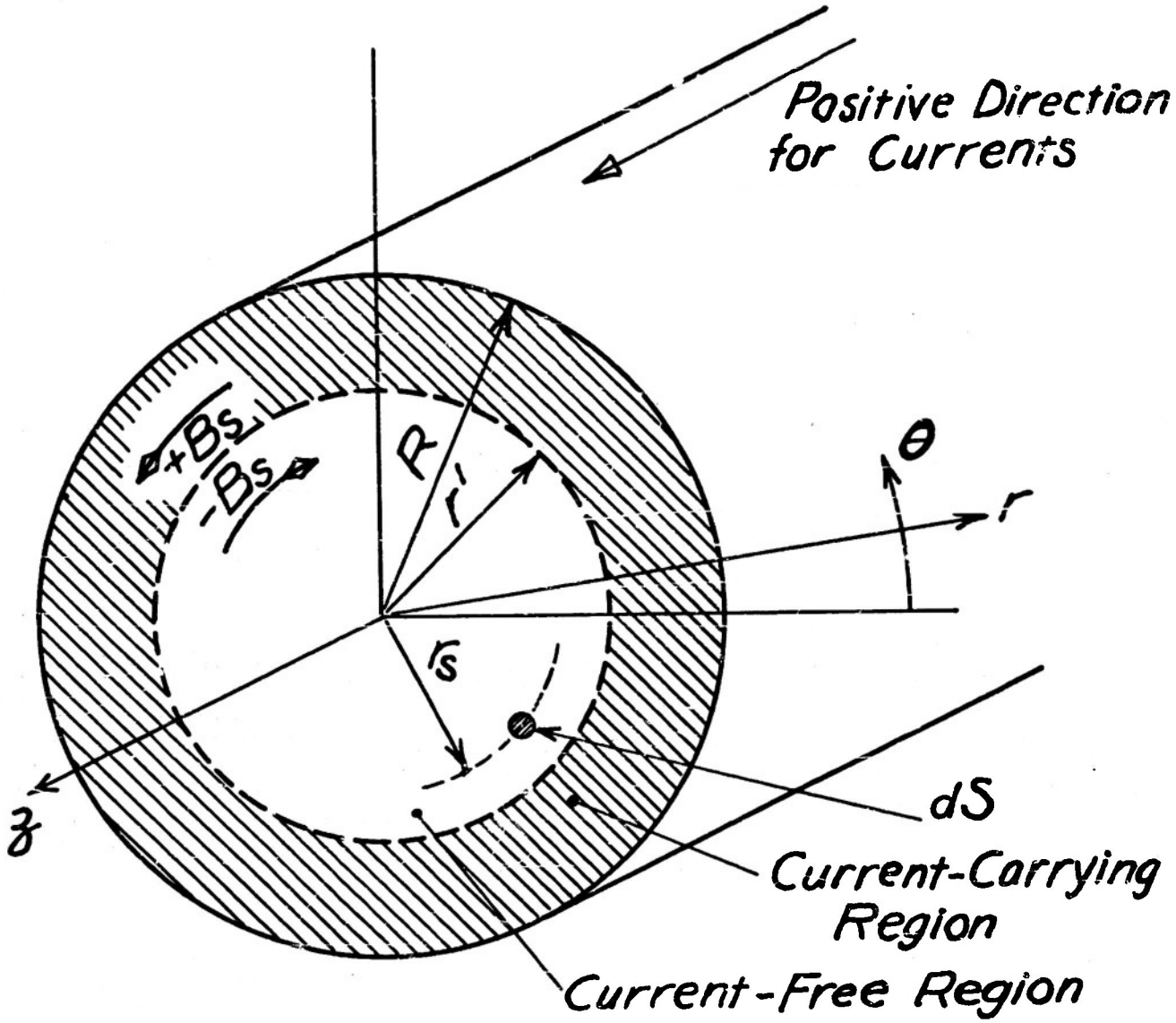
Positive Direction
for Currents
+Bs
-Bs
R
r'
θ
r
r̄s
z
dS
Current-Carrying
Region
Current-Free Region

Figure 6

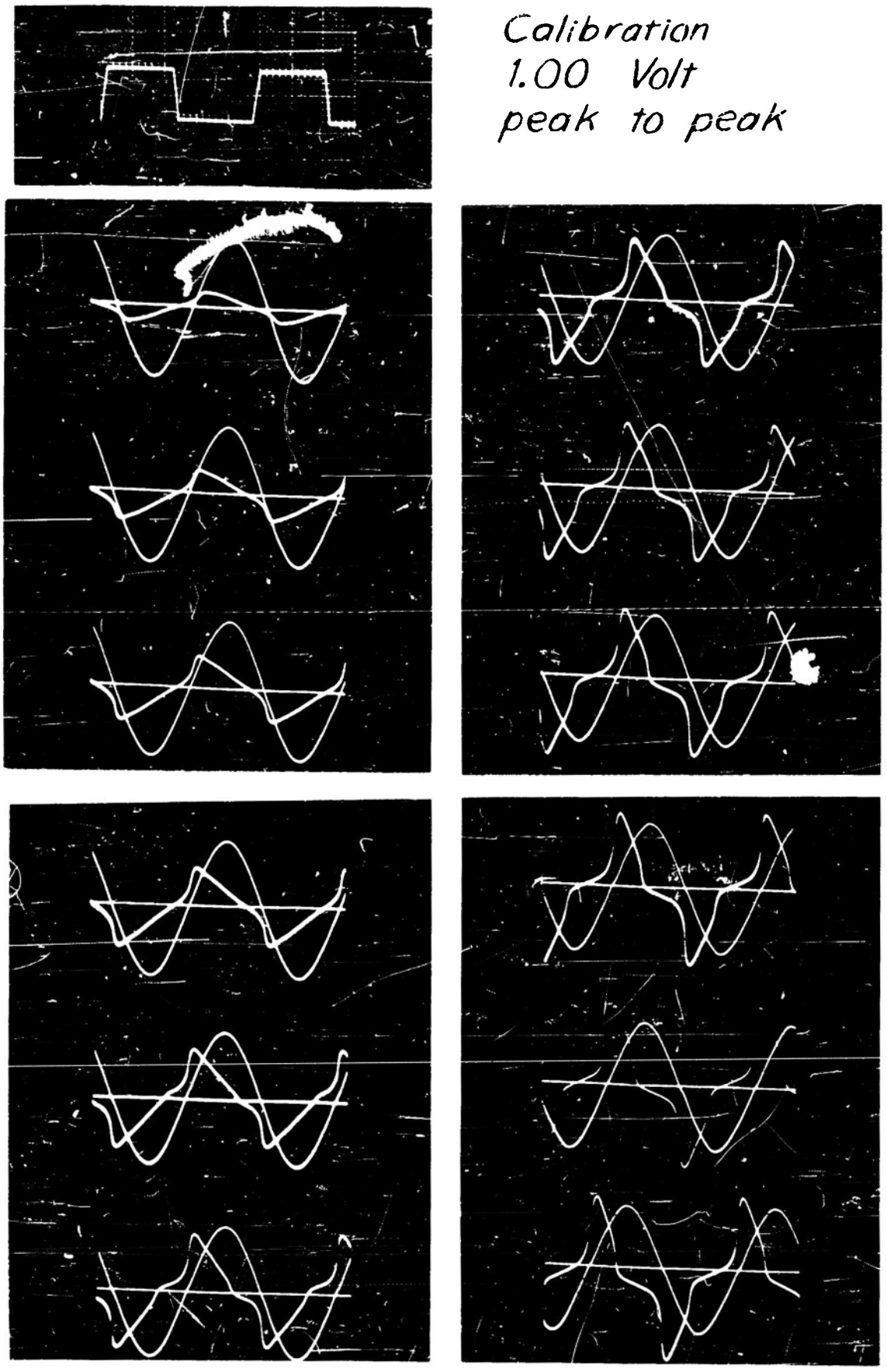

Figure 7
Hmm

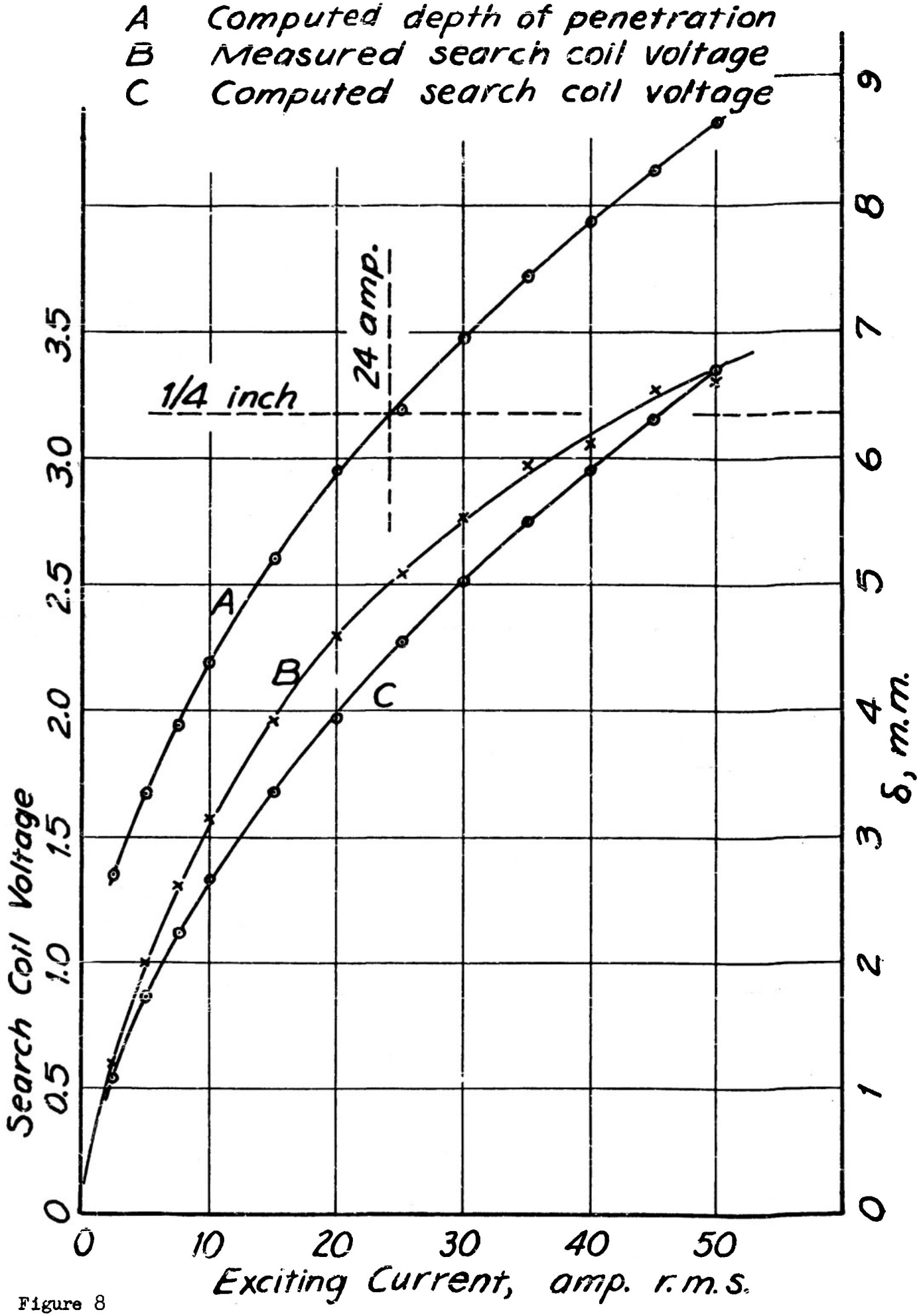
A Computed depth of penetration
B Measured search coil voltage
C Computed search coil voltage
1/4 inch
24 amp.
A
B
C
Search Coil Voltage
0
0.5
1.0
1.5
2.0
2.5
3.0
3.5
δ, m.m.
0
1
2
3
4
5
6
7
8
9
0
10
20
30
40
50
Exciting Current, amp. r.m.s.

Figure 8